REPORT DOCUMENTATION PAGE

Form Approved
OMB No. 0704-0188

PLEASE DO NOT RETURN YOUR FORM TO THE ABOVE ORGANIZATION.

1. REPORT DATE *(DD-MM-YYYY)*	2. REPORT TYPE	3. DATES COVERED *(From - To)*
20-11-2012	FINAL	March 15, 2009 to May 27, 2012

4. TITLE AND SUBTITLE

(YIP-09) Spatio-Temporal Characteristics of Scalar Mixing and Dissipation Processes in Turbulent Jets and Flames

5a. CONTRACT NUMBER

5b. GRANT NUMBER

FA9550-09-1-0272

5c. PROGRAM ELEMENT NUMBER

6. AUTHOR(S)

Jeffrey A. Sutton

5d. PROJECT NUMBER

5e. TASK NUMBER

5f. WORK UNIT NUMBER

7. PERFORMING ORGANIZATION NAME(S) AND ADDRESS(ES)

The Ohio State University
1960 Kenny Road
Columbus, OH 43210

8. PERFORMING ORGANIZATION REPORT NUMBER

9. SPONSORING/MONITORING AGENCY NAME(S) AND ADDRESS(ES)

Air Force Office of Scientific Research
875 N. Randolph St. Room 3112
Arlington, VA 22203
Dr. Chiping Li/RSA

10. SPONSOR/MONITOR'S ACRONYM(S)

11. SPONSOR/MONITOR'S REPORT NUMBER(S)

AFRL-OSR-VA-TR-2012-1203

12. DISTRIBUTION/AVAILABILITY STATEMENT

Distribution A: Approved for Public Release

13. SUPPLEMENTARY NOTES

14. ABSTRACT

The research objective of this program is to investigate the time-varying dynamics of scalar mixing relevant to turbulent reacting flows. Specifically, the program targeted the development and application of a new class of high-repetition-rate laser-based diagnostics to measure the time-varying mixture fraction, temperature, and species concentration fields in turbulent non-reacting jets and non-premixed flames. The result of the program was five new high-speed imaging techniques that were previously unavailable. High-speed planar Rayleigh scattering was developed to measure mixture fraction and temperature fields in turbulent jets and flames; high-speed spontaneous Raman scattering was developed to measure the temporal development of major species concentrations and the mixture fraction in reacting flows; and high-speed CH and CH2O PLIF were developed to monitor the time-varying, two-dimensional field of combustion intermediate and radicals with varying levels of reactivity. Targeted applications include understanding the time-dependent interaction between the large-scale turbulence and the small-scale mixing and species pro

15. SUBJECT TERMS

Turbulent flames; laser diagnostics; high-speed imaging, mixture fraction, temperature, species concentrations, Rayleigh scattering, Raman scattering, planar laser-induced fluorescence, mixing

16. SECURITY CLASSIFICATION OF:			17. LIMITATION OF ABSTRACT	18. NUMBER OF PAGES	19a. NAME OF RESPONSIBLE PERSON
a. REPORT	b. ABSTRACT	c. THIS PAGE			Dr. Chiping Li
U	U	U	U		19b. TELEPHONE NUMBER *(Include area code)* 703-696-8574

Reset

Standard Form 298 (Rev. 8/98)
Prescribed by ANSI Std. Z39.18

INSTRUCTIONS FOR COMPLETING SF 298

1. REPORT DATE. Full publication date, including day, month, if available. Must cite at least the year and be Year 2000 compliant, e.g. 30-06-1998; xx-06-1998; xx-xx-1998.

2. REPORT TYPE. State the type of report, such as final, technical, interim, memorandum, master's thesis, progress, quarterly, research, special, group study, etc.

3. DATES COVERED. Indicate the time during which the work was performed and the report was written, e.g., Jun 1997 - Jun 1998; 1-10 Jun 1996; May - Nov 1998; Nov 1998.

4. TITLE. Enter title and subtitle with volume number and part number, if applicable. On classified documents, enter the title classification in parentheses.

5a. CONTRACT NUMBER. Enter all contract numbers as they appear in the report, e.g. F33615-86-C-5169.

5b. GRANT NUMBER. Enter all grant numbers as they appear in the report, e.g. AFOSR-82-1234.

5c. PROGRAM ELEMENT NUMBER. Enter all program element numbers as they appear in the report, e.g. 61101A.

5d. PROJECT NUMBER. Enter all project numbers as they appear in the report, e.g. 1F665702D1257; ILIR.

5e. TASK NUMBER. Enter all task numbers as they appear in the report, e.g. 05; RF0330201; T4112.

5f. WORK UNIT NUMBER. Enter all work unit numbers as they appear in the report, e.g. 001; AFAPL30480105.

6. AUTHOR(S). Enter name(s) of person(s) responsible for writing the report, performing the research, or credited with the content of the report. The form of entry is the last name, first name, middle initial, and additional qualifiers separated by commas, e.g. Smith, Richard, J, Jr.

7. PERFORMING ORGANIZATION NAME(S) AND ADDRESS(ES). Self-explanatory.

8. PERFORMING ORGANIZATION REPORT NUMBER. Enter all unique alphanumeric report numbers assigned by the performing organization, e.g. BRL-1234; AFWL-TR-85-4017-Vol-21-PT-2.

9. SPONSORING/MONITORING AGENCY NAME(S) AND ADDRESS(ES). Enter the name and address of the organization(s) financially responsible for and monitoring the work.

10. SPONSOR/MONITOR'S ACRONYM(S). Enter, if available, e.g. BRL, ARDEC, NADC.

11. SPONSOR/MONITOR'S REPORT NUMBER(S). Enter report number as assigned by the sponsoring/ monitoring agency, if available, e.g. BRL-TR-829; -215.

12. DISTRIBUTION/AVAILABILITY STATEMENT. Use agency-mandated availability statements to indicate the public availability or distribution limitations of the report. If additional limitations/ restrictions or special markings are indicated, follow agency authorization procedures, e.g. RD/FRD, PROPIN, ITAR, etc. Include copyright information.

13. SUPPLEMENTARY NOTES. Enter information not included elsewhere such as: prepared in cooperation with; translation of; report supersedes; old edition number, etc.

14. ABSTRACT. A brief (approximately 200 words) factual summary of the most significant information.

15. SUBJECT TERMS. Key words or phrases identifying major concepts in the report.

16. SECURITY CLASSIFICATION. Enter security classification in accordance with security classification regulations, e.g. U, C, S, etc. If this form contains classified information, stamp classification level on the top and bottom of this page.

17. LIMITATION OF ABSTRACT. This block must be completed to assign a distribution limitation to the abstract. Enter UU (Unclassified Unlimited) or SAR (Same as Report). An entry in this block is necessary if the abstract is to be limited.

Final Report

SPATIO-TEMPORAL CHARACTERISTICS OF SCALAR MIXING AND DISSIPATION PROCESSES IN TURBULENT JETS AND FLAMES

(Grant Number: FA9550-09-1-0272)

Submitted By:

Jeffrey A. Sutton

Department of Mechanical and Aerospace Engineering

The Ohio State University

Columbus, OH 43210

Phone: 614-688-4999

Fax: 614-292-3163

E-Mail: sutton.235@osu.edu

I. Summary/Overview

The research objective of this program is to investigate the time-varying dynamics of scalar mixing relevant to turbulent reacting flows. Specifically, the principle investigator targeted the development and application of a new class of high-repetition-rate laser-based diagnostics to measure the time-varying mixture fraction, temperature, species concentration, and scalar gradient fields in turbulent non-reacting jets and non-premixed flames. While the initial scope of the project focused on an equal blend of measurement development and application, the program ended up heavily weighted toward developing and optimizing new measurement capabilities. This was deemed necessary to ultimately answer the most fundamental questions posed prior to the initiation of the project period.

The result of the program was five new high-speed imaging techniques that were previously unavailable. High-speed planar Rayleigh scattering was developed to measure mixture fraction and temperature fields in turbulent jets and flames, respectively; high-speed spontaneous Raman scattering was developed to measure the temporal development of major species concentrations and the mixture fraction in reacting flows; high-speed CH and CH_2O PLIF were developed to monitor the time-varying, two-dimensional field of combustion intermediate and radicals with varying levels of reactivity.

Subsequent to development, these techniques have been used to investigate the dynamics of turbulent mixing and species transport and will yield unique temporal and spatial statistics that augment direct visualization of the scalar mixing and transport dynamics. Targeted applications include understanding the time-dependent interaction between the large-scale turbulence and the small-scale mixing; the interaction between large-scale turbulence and species production/destruction; and the support of large-eddy simulation (LES) as a method of modeling ***time-varying*** turbulent combustion by providing new temporally-based visualization and statistical metrics for assessing model performance.

This work resulted in five previously-unavailable imaging techniques, seven archival journal papers, twelve conference papers and presentations, and eight additional invited seminars and talks. The technical accomplishments are expected to be useful to the general interests of AFOSR with specific interests expected in new measurement capabilities (of combustion dynamics) that can be applied to highly turbulent and high-Reynolds number combustion systems.

II. Introduction and Motivation

The United States Air Force devotes significant effort in fundamental propulsion research with the goal of developing systems such as scramjets, pulse detonation engines, and advanced gas turbine engines. The development of state-of-the-art air-breathing engines and propulsion systems requires novel measurement techniques capable of resolving governing physical and chemical processes under highly turbulent, high-Reynolds number, chemically-reacting flow conditions. Since turbulent combustion is the key phenomena in the majority of Air Force propulsion systems, detailed measurements under relevant conditions are critical for assisting engine/aircraft designers in optimizing propulsion systems, investigating challenging performance problems, and assessing and validating computational models such as large-eddy simulations (LES) and the underpinning assumptions that could greatly reduce prototyping time and costs.

Turbulent flows are inherently time-varying, multi-dimensional phenomena, and when coupled to chemical reactions, create a highly dynamic system occurring on multiple length and time scales. Current combustion models have difficulty in accurately predicting the time-dependent coupling between the turbulent fluid mechanics, scalar mixing and transport, and finite-rate chemistry over a broad range of conditions. The lack of *robust* and *predictive* modeling capabilities dictates that the primary assumptions underpinning combustion models need to be assessed, with carefully-designed experiments playing a crucial role in detailing the combustion dynamics. Recognizing that turbulence and turbulent combustion processes are inherently stochastic, scalar mixing and transport processes must be resolved in both space and time in order to capture the dynamic nature of these flows. This requirement dictates that the data acquisition of two- and three-dimensional fields is at much faster rates than typical time-scales of the turbulent processes (>> 1 kHz). Non-intrusive optical methods have the potential to resolve pertinent chemical and physical processes at the smallest length and time scales; however new experimental tools are required to provide currently unavailable data that is both spatially- and temporally-resolved.

Over the last three years, the principle investigator has been engaged in the development of advanced high-speed laser diagnostic measurements in turbulent combustion environments, with a specific interest in developing and applying new measurement techniques to examine previously-inaccessible turbulence and combustion dynamics. As significant portion of this

research program was devoted to the development of high-repetition-rate Rayleigh scattering, Raman scattering, and planar laser-induced fluorescence (PLIF) diagnostics to image the time-varying mixture fraction, temperature, and species concentrations fields in turbulent jets and non-premixed and partially-premixed flames for the first time. This research laid the groundwork for developing a better fundamental understanding of the physics governing the highly, unsteady turbulent mixing and scalar transport processes within combustion environments. In addition, the new measurement capabilities support large-eddy simulation (LES) as a method of modeling time-varying turbulent combustion by providing new structural/dynamic information as well as more suitable temporally-based statistical metrics for assessing the predictive capabilities of LES models.

III. Overview of Accomplishments

The present research program was experimental in nature, but also resulted in synergistic activities with computational researchers. Excellent progress was made in the area of high-speed imaging development and satisfactory progress is currently being made in investigating the physical dynamic mechanisms governing scalar mixing and transport (in turbulent flows and flames)[1]. The research program resulted in seven archival journal papers, twelve conference papers and presentations, and eight additional invited seminars and talks. Highlights of the previous accomplishments are detailed in previous annual reports and presentations as well as the published journal and conference papers. In this manner, only a brief summary of the work performed under the present research program will be given; for a detailed description of the work, the reader is referred to the individual published papers.

1. Pulse Burst-Mode Imaging

Recently, high-speed imaging in combustion environments has been made possible by advances in diode-pumped, solid-state (DPSS) lasers and CMOS-based camera systems. While the emergence of commercially-available laser systems has certainly been exciting, the low pulse energies (a few milliJoules) currently limit the diagnostic techniques that may be employed in combustion environments. Previously, only particle imaging velocimetry (PIV) and OH planar

[1] Research using the newly developed high-speed diagnostics aimed at understanding the time-dependent nature of scalar mixing and dissipation will continue beyond the current grant period and at no cost to the current program.

laser-induced fluorescence (PLIF) have been used heavily as indicated in a recent review paper by Böhm et al. [1]. Other techniques including planar Rayleigh scattering or spontaneous Raman scattering imaging, which are required to measure important scalars such as temperature and mixture fraction in turbulent combustion environments [e.g., 2], require very high pulse energies and are essentially prohibited by the low pulse energies of commercially-available DPSS lasers. Similarly, many other important combustion radicals such as CH, O, H, or NO cannot be easily imaged using planar laser-induced fluorescence (PLIF) because the UV laser energy obtained using commercial systems is too low.

In order to overcome some of these limitations, the PI and his group use an alternative approach; that is, pulse-burst laser technology [3] is used to generate a series of high-energy laser pulses in rapid succession to extend the number of laser-based measurements that may be performed at kHz (to MHz) acquisition rates. In this section, a new high-energy pulse burst laser system (HEPBLS) recently developed at Ohio State is described [4]. It is noted that this laser system was developed and constructed at no cost to AFOSR, but was leveraged in the PI's AFOSR-supported research program. This system produces an unprecedented combination of high-repetition-rates, high pulse energies, and long pulse sequences to allow quantitative high-repetition rate imaging in turbulent combustion environments that has not been available previously. **This approach, which involves generating hundreds of sequential pulses at high repetition rates, is advantageous (or even necessary) for imaging highly turbulent flows.**

A schematic of the custom HEPBLS is shown in Fig. 1a. The HEPBLS was designed to produce a unique combination of high repetition rates and high pulse energies over long pulse burst durations (high average power) for quantitative time-resolved imaging of turbulence and combustion dynamics. Briefly, the HEPBLS is a master oscillator-power amplifier (MOPA) system that amplifies the low-energy output (~10 μJ/pulse) of a continuously running single-frequency Nd:YVO_4 laser (which serves as the oscillator) in a series of long-duration, flashlamp-pumped Nd:YAG amplifiers. Between amplification stages, there are several subtle, but important, system attributes aimed at controlling unwanted birefringence, diffraction, and thermal lensing effects and preserving high beam quality, which is important for the high energy and power output of the current system. Beyond simple spatial filtering, the output of each amplifier is "imaged" onto the exit plane of the subsequent amplifier through relay optics and in the case of the final stages (4 and 5), vacuum relay optical setups. Each relay station consists of

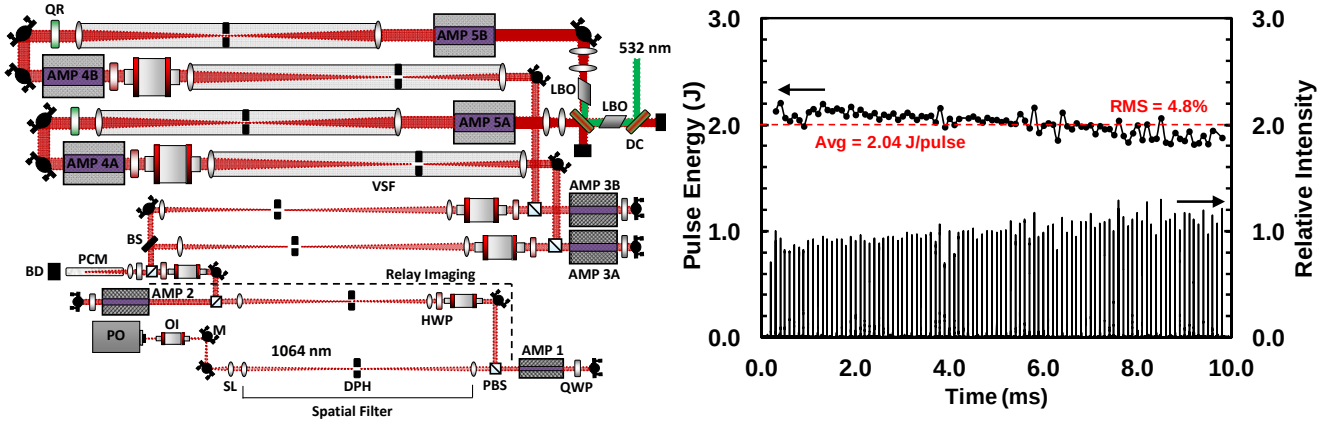

Fig. 1 – (a) Schematic of HEPBLS at OSU. (b) Example pulse burst intensity trace and pulse energy distribution within a single 10-ms burst. The standard deviation of the energy fluctuation is < 5%.

a set of lens pairs that focus the beam through an additional "low-pass" spatial filter (diamond pinhole which is ~10 times the diffraction-limited spot size [5]) and re-collimates the light at the desired magnification. Such a process suppresses diffraction ripples and helps to cancels birefringence effects at each stage.

After two stages of amplification, the output energy (or more appropriately the intensity) is high enough for efficient retro-reflection from a Stimulated Brillouin Scattering (SBS)-based Phase Conjugate Mirror (PCM) [6]. The PCM serves to break up what is known as Amplified Spontaneous Emission (ASE), an undesirable effect which limits achievable gain and grows exponentially with the number of amplification stages. After the PCM the pulse train is split into two parallel legs ("A" and "B"), each of which contains three additional dual-flashlamp-pumped amplifiers with Nd:YAG rod diameters of 9.5 mm (AMP 3) and 19 mm (AMP 4 and AMP 5). AMP3 is configured for double-pass amplification, while AMP4 and AMP 5 of each leg are operated in a single-pass configuration with a 90-degree quartz rotator placed between the two amplifiers to mitigate thermally-induced birefringence. The parallel leg design allows for a delay in gain saturation in the final amplifier stages and leads to a higher total output energy for equivalent levels of individual stage gain. The total gain for AMP 3, 4, and 5 is greater than 30 and the total gain for the system is greater than 10^5.

The repetition rate of the master oscillator (specified up to 250 kHz) determines the pulse spacing within the burst, while the flashlamp discharge duration determines the overall length of the burst and the number of amplified pulses. The current system is designed to discharge for

more than 25 ms per burst and we have tested the system successfully up to 20 ms. At 10 kHz (100 μs spacing), this corresponds to 200 high-energy pulses, which is quite extraordinary considering that the final energies are **> 2 Joules/pulse** at 1064 nm [4] with an RMS of the pulse-to-pulse fluctuation within the burst is less than 5% (see Fig. 1b). The record lengths are more than sufficient to characterize the time-varying behavior of turbulent flowfield-flame interactions both visually and statistically as well as being well-match to typical LES simulation times (10's of milliseconds). Finally, the fundamental, 1064-nm output of the HEPBLS is frequency-doubled to 532 nm for high-speed Rayleigh and Raman scattering imaging and frequency-tripled to 355 nm for high-speed PLIF imaging. Second harmonic generation conversion efficiency as high as 60% has been achieved using two type I LBO crystals (12 x 12 x 20 mm^3) in series.

2. High-Speed Mixture Fraction Imaging in Turbulent Jets

The mixture fraction ξ is the most fundamental (and perhaps the most important) scalar in non-premixed and partially-premixed combustion. The turbulent mixing field can be uniquely characterized by ξ, and for many combustion models, the turbulent flame structure can be related back to ξ and its derivatives. Practically speaking, for a large class of combustion systems, the rate at which the fuel and oxidizer mix governs the rate of chemical reaction and under highly turbulent conditions, it is highly desired to track its evolution in both space and time. A key focus of the experimental program was to measure the mixture fraction field, $\xi(x,t)$, in turbulent non-reacting jets to first understand scalar mixing dynamics in the absence of chemical reaction and exothermic heat release.

The mixture fraction fields in turbulent non-reacting jets were measured using planar Rayleigh scattering. Rayleigh scattering (LRS) is a non-intrusive diagnostic that describes the scattering from atoms and molecules whose effective diameter is much less than the wavelength of the incident light. For low-repetition rate studies, planar Rayleigh scattering is a widely-used imaging technique for mixture fraction measurements in non-reacting flows because of the high measurement sensitivity that may be achieved by issuing a fluid with a large Rayleigh scattering cross section into another fluid with a much lower scattering cross section, i.e., propane into air [e.g. 7-9].

The total Rayleigh scattering intensity can be written as

$$I_{RAY} = AI_o n\sigma_{mix} \quad (1)$$

where A is a constant describing collection volume and efficiency of the optical setup, I_o is the incident laser intensity, n is the number density, and σ_{mix} is the mixture-averaged differential cross-section defined as $\sigma_{mix} = \sum_{i=1}^{N} X_i \sigma_i$. X_i and σ_i are the mole fraction and differential cross-section of species i, respectively. For a flow that is isothermal and isobaric, changes in the scattered intensity, I_{RAY} are due to variations in σ_{mix}. For a two-stream mixing process (jet fluid issuing into air), Eq. (1) can be re-written as

$$I_{RAY} = KI_o n[X_J \sigma_J + (1 - X_J)\sigma_A] \quad (2)$$

where X_J is the mole fraction of the jet fluid at any point in the flow, σ_J is the differential cross-section of the jet fluid, and σ_A is the differential cross-section of air. Equation (2) can be re-arranged such that the local mole fraction of the jet-fluid (X_J) is determined from the Rayleigh scattering signal (I_{RAY}) at any point in the flow and measured calibration signals from pure jet-fluid (I_J) and pure air (I_A):

$$X_J = \frac{I_{RAY} - I_A}{I_J - I_A} \quad . \quad (3)$$

Subsequently, the mixture fraction is determined from

$$\xi = \frac{Y_J}{Y_{J,0}} = \frac{X_J W_J}{X_J W_J + (1 - X_J) W_A} \quad (4)$$

where Y_J is the mass fraction of the jet fluid at any point in the flow, and $Y_{J,0}$ is the mass fraction of the jet fluid originating from the source ($Y_{J,0} = 1$), W_J is the molecular weight of the jet fluid, and W_A is the molecular weight of the air.

Although frequently utilized at low repetition rates, planar Rayleigh scattering requires pulse energies that currently are not available from commercial high-repetition-rate laser systems. However, the new HEPBLS, developed during the AFOSR funding period, allows high-speed (multi-kilohertz) planar Rayleigh scattering imaging.

For the high-speed mixture fraction imaging, a turbulent propane jet issuing into a co-flowing stream of air was considered. The propane issued from an 8-mm-diameter circular tube into a 300 mm x 300 mm co-flowing stream of air. Four cases were considered where the propane exits the tube at Reynolds numbers of 10,000, 15,000, 20,000, and 30,000 based on tube

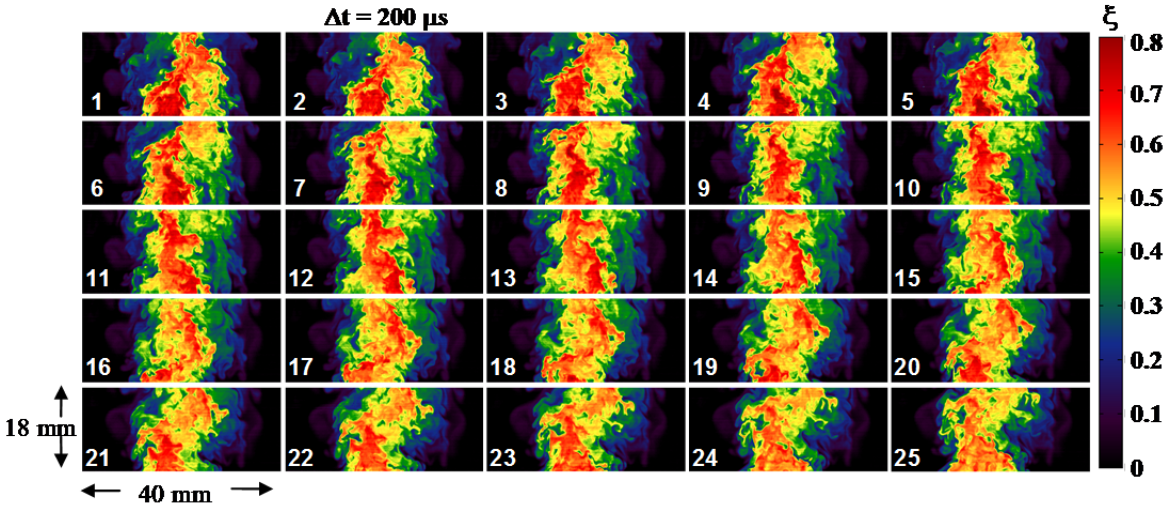

Fig. 2 – 25-frame (of 100), 5-kHz sequence of the mixture fraction field in a turbulent (Re = 15000) non-reacting propane jet issuing into air. Image sequences are shown for an axial position of x/d = 10. The images were acquired at 10 kHz, but only every other image (200 μs spacing) is shown for clarity. The total time represented is 5 ms.

diameter. Propane is chosen for its large Rayleigh scattering cross-section (approximately 13 times that of air), which results in a high signal-to-noise ratio for the acquired images.

As described in Ref. 10, a considerable amount of effort was devoted by the PI and his group on quantifying the measured signals using high-framing rate CMOS cameras. Although image processing for traditional CCD cameras is well-established, the characteristics of CMOS cameras are not well known and this infrastructure has to be developed. In contrast to well-characterized CCD sensors which have uniform pixel response and an exceptionally high degree of sensor linearity, CMOS sensors have the potential to have an independent, non-linear response for each pixel [11] because each pixel in a CMOS sensor acts as an independent active circuit. Recent papers [11, 12] focusing on the linearity and uniformity of CMOS cameras have appeared in the literature demonstrating the need to carefully calibrate CMOS cameras for quantitative measurements. While this may seem as a minor point within an experimental program, it cannot be under-estimated the effort that it takes to characterize performance characteristics of newer technology such as CMOS-based cameras. In this manner, the work performed by the PI and his group in this area will be far-reaching, especially as more and more research groups transition into high-speed measurements and these measurements are used to assess turbulence and combustion models such as LES.

Figure 2 shows an example data series taken from high-repetition-rate Rayleigh scattering measurements of a turbulent propane jet (Re = 15,000) issuing into a co-flowing stream of air at

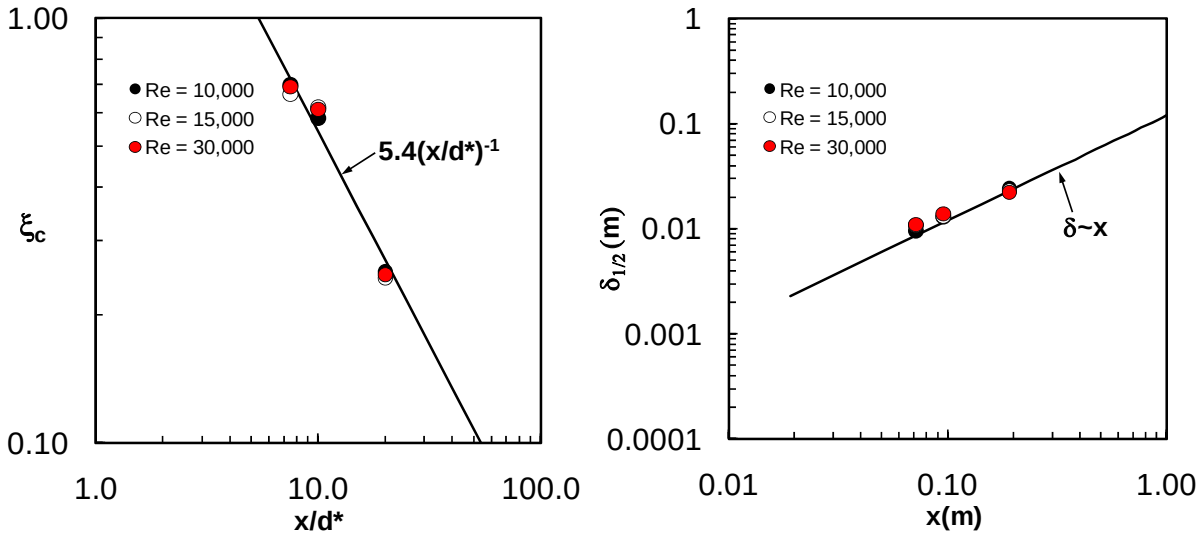

Fig. 3 – Comparison between measured mean centerline mixture fraction, ξ_c and mixture fraction scaling laws for a turbulent jet. (b) Comparison between measured jet-half-width (δ) and scaling laws for a turbulent jet. Note, three Reynolds number conditions are reported at each axial position.

an axial position of x/d = 10, where *d* is the nozzle diameter. The high-energy output of the new HEPBLS was used at 10 kHz to obtain this image sequence. The high signal-to-noise ratio (SNR > 100 in the core) and resolved small-scale features are quite evident; in fact, the spatial resolution and image SNR are sufficiently high to enable high quality determination of the scalar dissipation rate, $\chi \sim (\nabla\xi \bullet \nabla\xi)$, which characterizes the rate of molecular mixing. However, the significance of the mixture fraction images lies beyond the spatial quality, that is, the utility of the images is evidenced in the temporal correlation of the images and the ability to track turbulent mixing dynamics in real time. As an example, the evolution of the mixing field topology and the dissipation of small-scale scalar structures are clearly seen, thereby displaying the time-varying nature of turbulent mixing and the steep concentration gradients that turbulent mixing introduces. This work (as published in [10] and an upcoming submission [13]) represents the first sets of temporally-correlated (quantitative) measurements of the mixture fraction fields in highly turbulent gaseous jets.

An assessment of the accuracy of the mixture fraction measurements is made by comparing both the mean value of the centerline mixture fraction, ξ_c, and the jet width for all three Reynolds number cases and axial positions to known scaling laws for turbulent jets. The mean values are determined from 200 individual (non-correlated) images (taken from the high-speed image

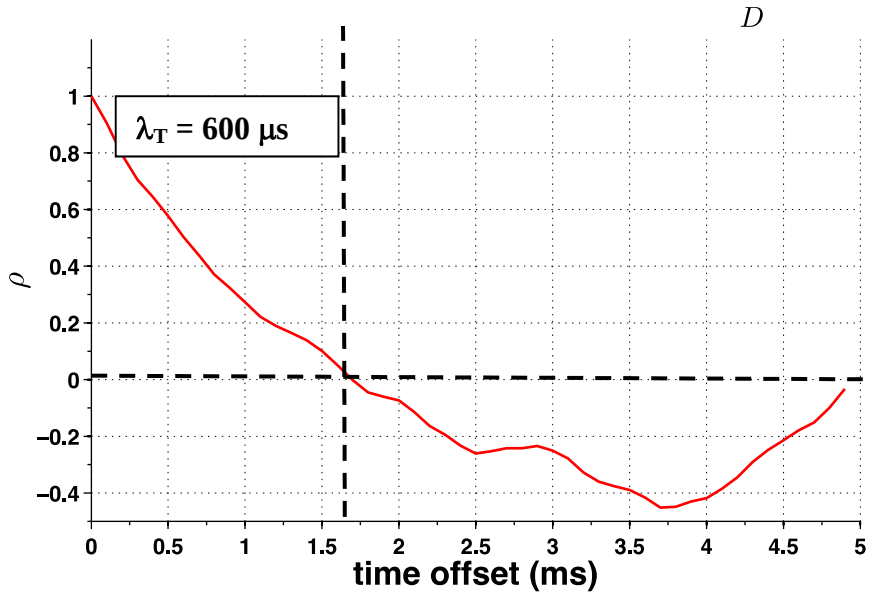

Fig. 4 – Example temporal correlation function for a turbulent (Re = 15000) jet at x/d = 15. The integral time scale is determined as ~600 μs.

sequences) per Reynolds number per axial distance. As discussed by Tacina and Dahm [14], the centerline value of the mixture fraction is expected to scale as:

$$\xi_c(x) = 5.4(x/d^*)^{-1} \qquad (5)$$

where x is the axial distance downstream of the exit nozzle and d^* is the "momentum diameter" which accounts for differences in density between the jet fluid and the ambient air, i.e., $d^*=(\rho_{jet}/\rho_{air})^{1/2}d$, where d is the nozzle diameter. In addition, the jet-width (e.g., the "outer length scale") can be expected to scale as $\delta(x) \sim x$, where the constant is determined from experimental data and the specific definition of the jet-width. Figures 3(a) and 3(b) show that both the mean centerline mixture fraction (ξ_c) and jet half-width measured using the high-speed Rayleigh scattering diagnostic compare very favorably to the turbulent jet scaling laws for all three Reynolds number conditions, thereby providing an initial validation of the accuracy of the mixture fraction measurements, at least for the present experimental conditions.

The most recent work has focused on using the new high-speed mixture fraction imaging capability to characterize turbulent mixing dynamics including (i) integral time scales as a function of axial position and Reynolds numbers, (ii) power spectra, and (iii) temporal fluctuations and correlations between mixture fraction and scalar dissipation rate. As one example of the utility of these measurements, Fig. 4 shows an example of the temporal

correlation function (ρ) on centerline at an axial position of x/d = 15 for the Re = 15,000 jet. The integral time scale is calculated as

$$\lambda_T = \int \rho(\tau) d\tau \ . \qquad (6)$$

which for the present example yields a value of 600 μs. While this analysis can be considered preliminary, this data represents the first measurements to determine the integral time scale of the mixture fraction field in gas-phase flows using optical diagnostics.

3. High-Speed Temperature Imaging in Turbulent Flames

Within a turbulent combustion environment, temperature is a very important scalar. For non-premixed combustion, the thermal field is inherently linked and strongly correlated with the mixture fraction field in flame cases far from extinction. Thus thermal gradients and dissipation structures derived from the temperature field not only yield physical information on the thermal mixing, but on the underlying structure of the molecular mixing processes as well [e.g., 15, 16]. In turbulent premixed combustion systems, the temperature field yields a distinction between reactants and products and can be converted to the characteristic reaction progress variable (c_T), which underpins many turbulent premixed flame models and yields direct insight into the internal structure of the premixed flames. Furthermore, local reaction rates and pollutant formation can be strongly temperature-dependent and thus it is important to measure the local temperature field and it is highly desired to measure its temporal fluctuation.

Within this program, the PI and his research group demonstrated the first high-speed temperature imaging in turbulent flames [17] and have continued to improve the capabilities using the new HEPBLS. High-speed planar Rayleigh scattering was used to measure the local temperature field in the flames. For low Mach number flows, the ideal gas law, $p = nkT$, where p is the pressure, k is the Boltzmann constant, and T is the temperature can be can be used in association with Eq. (1) to relate measured intensity to local gas temperature:

$$I_{RAY} = AI_o \frac{P}{kT} \sigma_{mix} \qquad . \qquad (7)$$

For flame temperature measurements, the constant A is typically accounted for by normalizing the measured Rayleigh signal to a Rayleigh signal of known temperature and species concentration such as that from air at room temperature. If the differential Rayleigh scattering cross section is constant across the flame, the temperature is derived from

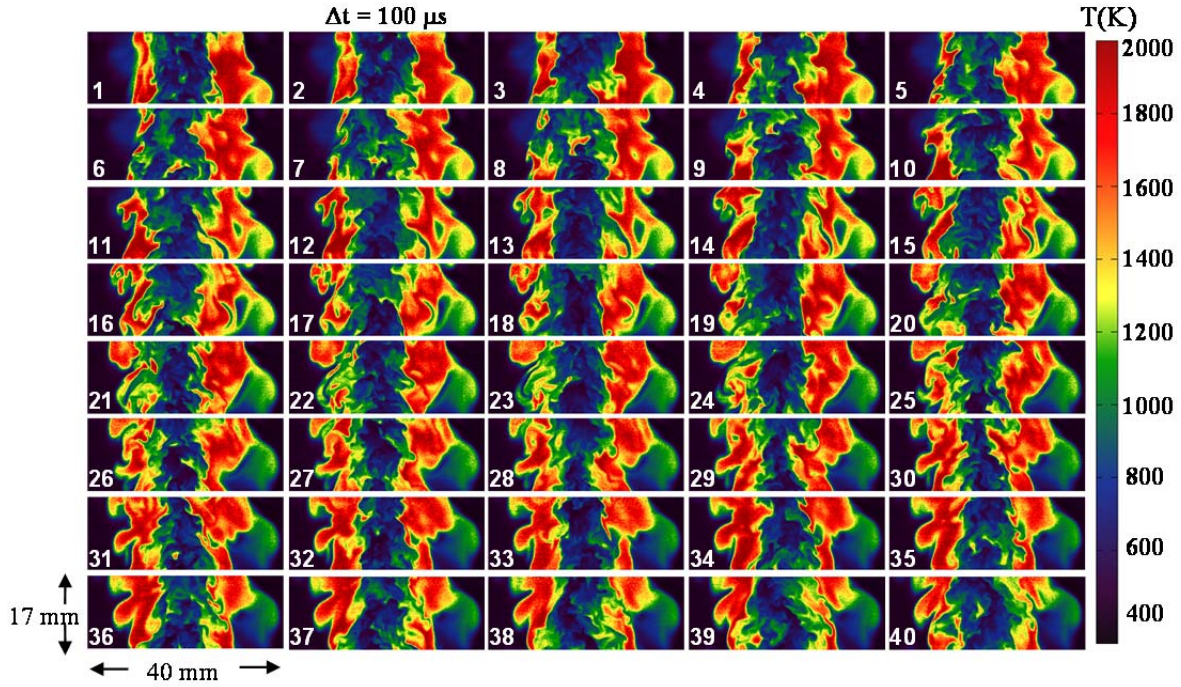

Fig. 5 – 40-frame (of 100), 10-kHz sequence of the temperature field in a turbulent (Re = 22800) non-premixed jet-flame issuing into air. Fuel mixture is 22.1% CH4 /33.2% H2 / 44.7% N2 and Re = 22,800 (DLR B Flame). Image sequences are shown for an axial position of x/d = 10. The total time represented is 4 ms.

$$T = T_{ref} \frac{I_{ref}}{I_{RAY}} \quad . \tag{8}$$

where I_{ref} is the reference Rayleigh scattering signal from air at room temperature (T_{ref}). The turbulent non-premixed flames considered in this study are the well-characterized DLR-A and DLR-B flames [18, 19] which are comprised of a fuel mixture of 22.1% CH_4, 33.2% H_2, and 44.7% N_2. For this fuel combination, the mixture-averaged differential cross-section varies by less than 3% throughout the flame, thus enabling a calculation of the local gas temperature without a need for measuring the local species concentrations.

The DLR flames considered in this study are simple jet-flames issuing into a low-speed co-flow of air (~0.3 m/s) that serve as benchmark flames in the International Workshop for the Computation of Turbulent Nonpremixed Flames (TNF Workshop) [20]. The fuel, which consists of 22.1% CH_4 /33.2% H_2 / 44.7% N_2, issues from a 8-mm-diameter tube at 43.2 m/s for DLR Flame A and 63.2 m/s for DLR Flame B into the 30 cm x 30 cm co-flow. These flow conditions correspond to Reynolds numbers of 15200 and 22800, respectively based on nozzle diameter.

Flame A displays low levels of local flame extinction, while Flame B is close to blowoff and displays moderate levels of local extinction [18].

Figure 5 shows an example of a recent 10-kHz temperature sequence obtained within a turbulent non-premixed flame operating at Re = 22,800. **500 mJ/pulse at 532 nm** was outputted from the HEPBLS, which allowed the use of a CMOS camera only (no image intensifier) for increased signal-to-noise ratio and spatial resolution. From the images, new features such as the formation of "flame holes" (cold gas pockets surrounded by hot gas) and the upstream propagation of a high-temperature reaction zone are clearly seen, showing the time-varying (dynamic) nature of thermal mixing and the introduction of steep thermal gradients. Image sequences, such as these, are providing a new understanding of turbulent thermal mixing and flame dynamics. Using Fig. 5 as an example, the formation of the flame holes, the rapid engulfment by hot gases, and the subsequent upstream propagation of hot gases appear to highlight a flame extinction/re-ignition mechanism. As noted in Fig. 5, the signal quality (signal-to-noise ratio, SNR) is quite high for these images. The SNR is approximately 40 and 17 for the low-temperature co-flow and high-temperature regions, respectively. Figure 6 shows an example temporal trace of temperature taken from the data set shown in Fig. 5 at three closely spaced positions near the high-temperature reaction zone. It is noted that significant thermal fluctuations are observed with temperatures fluctuating as much as 900 K in 100 μs (9×10^6 K/s).

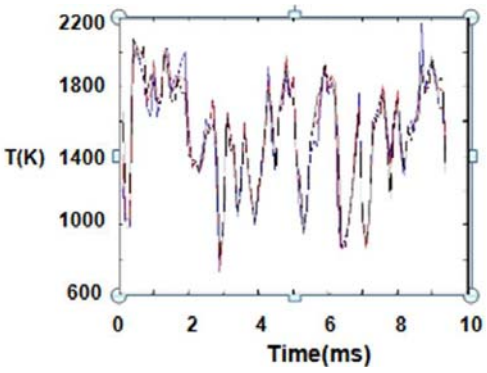

Fig. 6 – Example temporal trace of temperature (at 3 spatial locatioins) in DLR flame B. Temporal gradients as high as 9×10^6 K/s are noted.

To assess the accuracy of the high-speed temperature measurements, the time-averaged temperature field and root-mean square (RMS) of the temperature field at an axial position of x/d = 20 are computed and compared to the reference point-based data taken at Sandia National Laboratories, which appears as part of the TNF database for the DLR flames [20]. The TNF data was acquired with simultaneous Raman/Rayleigh scattering and CO laser-induced fluorescence measurements at an acquisition rate on the order of a few Hertz and spatial resolution of 750 μm. Approximately 1000 samples were acquired for each measurement location. For the current high-speed temperature imaging, the mean and RMS temperature values at a given spatial

location were extracted from the computed 2D mean and RMS temperature fields based on 120 images. Figure 7 shows the comparison between the current high-speed imaging data and the reference data from Sandia for both DLR flames A and B plotted against the normalized radial position (*r/d*). As shown in Fig. 7, there is very good agreement between the current high-speed imaging and Sandia reference data for the mean temperature values for both DLR flames, both in terms of temperature magnitude and radial profile shape (mean temperature gradient). In terms of the RMS temperature values, the overall profile shape is computed quite accurately for both flames A and B.

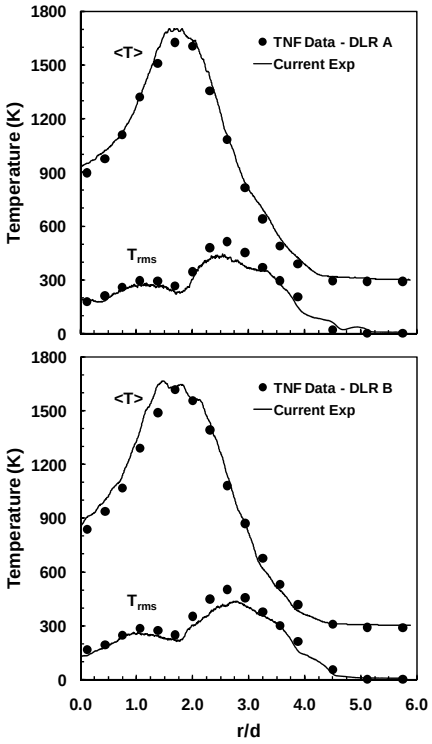

Fig. 7 – Comparisons of the time-averaged mean and RMS radial temperature profiles measured at an axial position of x/d = 20 in the DLR flames from current high-speed imaging (solid line) and the reference point data (symbols) from Sandia National Laboratories [20]. (*Top*) DLR flame A; (*Bottom*) DLR flame B.

4. High-Speed Raman Scattering Imaging in Turbulent Jets/Flames

A major focus of the current research program is the development of high-energy, high-repetition-rate diagnostics that can be used for 1D Raman scattering line imaging, thus permitting a measurement of the major species in both space and time and a measurement of $\xi(x,t)$ in turbulent flames [21]. An initial set of measurements demonstrating the first high-speed 1D Raman line imaging was performed in turbulent non-reacting CH_4/H_2 jets issuing into air [22] as shown in Fig. 8. This flow was chosen such that the major species encountered during combustion were present within the flow field. The 7-mm line profiles of CH_4, H_2, O_2, and N_2 are easily identified, although the first measurements showed modest signal-to-noise ratios.

Subsequently, the PI and his group have been examining system performance within combustion environments. To assess the accuracy of the high-speed, CMOS camera-based Raman imaging system, measurements were performed in a series of well-characterized, near adiabatic equilibrium, premixed, laminar flames. Figure 9 shows the measurement of the major combustion species (H_2, N_2, O_2, and H_2O) and temperature over a broad range of equivalence

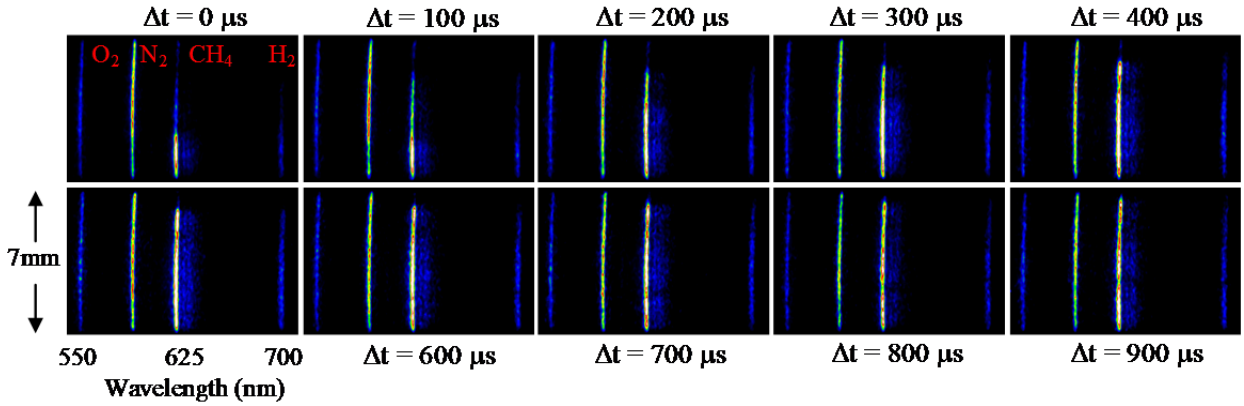

Fig. 8 – 10-kHz sequence of 1D Raman scattering images in a turbulent CH_4/H_2 jet issuing into a co-flowing stream of air. Images are centered at x/d = 10.

ratios. While the measurements were performed at low repetition rates (10 Hz), they were performed with the exact same optical and detection systems used for 10 kHz. It is noted that the results match equilibrium calculations very well over the full equivalence ratio space giving confidence in the ability to measure quantitative major species concentrations and mixture fraction profiles in turbulent flames.

Current work in the PI's lab is focusing on 10 kHz Raman scattering measurements in turbulent H_2/N_2 flames. The significance of realizing multi-kilohertz-rate imaging of $\xi(x,t)$ in turbulent flames cannot be under-stated as this will give direct insight concerning the transient mixing processes and dynamic turbulence-chemistry interactions in reacting flows that directly underpin engine performance and efficiency. In addition, the new measurements of $\xi(x,t)$ in turbulent flames will significantly augment the existing data sets available to LES modelers through temporally-correlated measurements and new temporal statistics such as joint temperature-mixture fraction, temperature-major species, major species-mixture fraction space-time correlations.

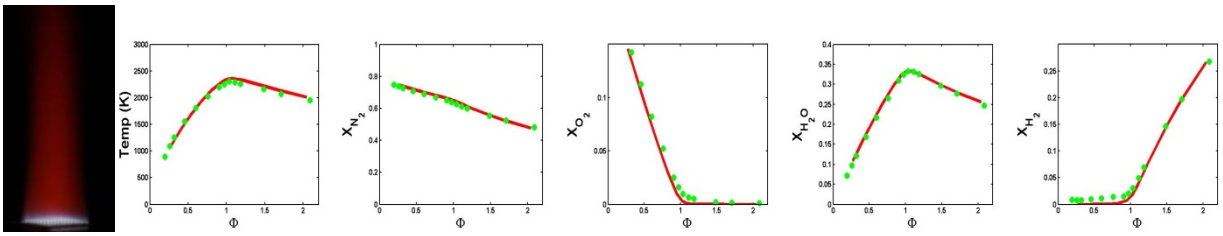

Fig. 9 – (*Left*) Photograph of a near-adiabatic premixed H_2-air flame. (*Right*) Measurements (green symbols) of temperature and major species as compared to equilibrium calculations (red lines).

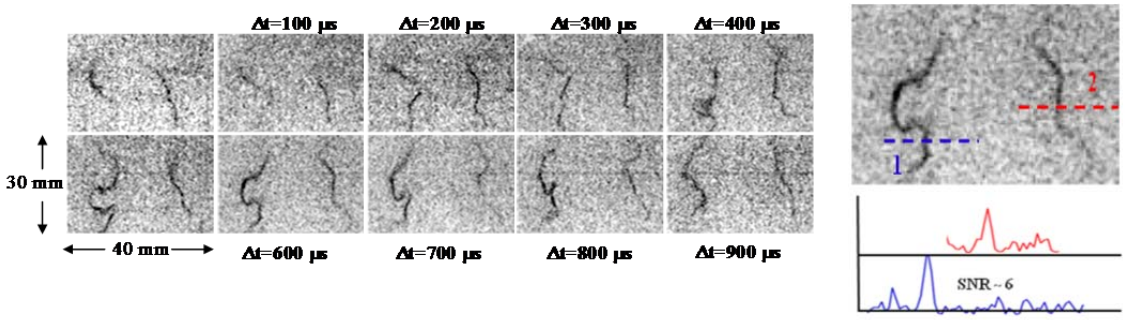

Fig. 10 – A ten-frame CH PLIF image sequence in DLR Flame A at an axial position of 175 mm downstream of burner exit. The spacing between the images is 100 μs, corresponding to a 10-kHz acquisition rate.

5. High-Speed CH and CH_2O Planar Laser-Induced Fluorescence

A final area of research in this program is the application of high-repetition rate PLIF imaging of combustion radicals and intermediates that cannot be performed using commercially-available laser systems. The output of the PBLS(s) can be frequency-tripled to 355 nm for pumping an optical parametric oscillator (OPO) as described in Ref. 23. The development of the PBLS-pumped OPO has allowed the generation of tunable visible and near-IR laser light that can be frequency-mixed with residual 1064 nm, 532 nm, or 355 nm output to produce tunable UV laser light for high-speed PLIF imaging. Previously this process has been demonstrated with NO PLIF imaging (at 226 nm) in non-reacting supersonic flows [24-26] and OH PLIF imaging (at 310 nm) in turbulent hydrogen-air flames [27]. In this program, we have extended the capabilities to cover CH PLIF imaging at 390 nm in turbulent hydrocarbon flames [28]. As an example of the utility of this measurement, the CH radical has long been considered an appropriate marker of the inner reaction zone in both non-premixed and premixed hydrocarbon flames since its location marks the final step in hydrocarbon fuel decomposition [e.g., 29]. Figure 10 shows an example of a ten-frame CH PLIF image sequence recorded in the DLR Flame A with 100-μs spacing between successive images, corresponding to a 10-kHz acquisition rate. The images were taken on centerline and at 175 mm above the fuel tube with 0.4 mJ/pulse. Figure 10 also shows two intensity profiles taken horizontally from image 7 of the CH PLIF sequence shown at the axial location specified with the two dashed lines. The SNR of the CH PLIF image at both of these axial locations is approximately 6.

Formaldehyde (CH_2O) is an important combustion intermediate occurring within the "cool flame" region prior to the primary reaction zone. CH_2O is a key species in low-temperature

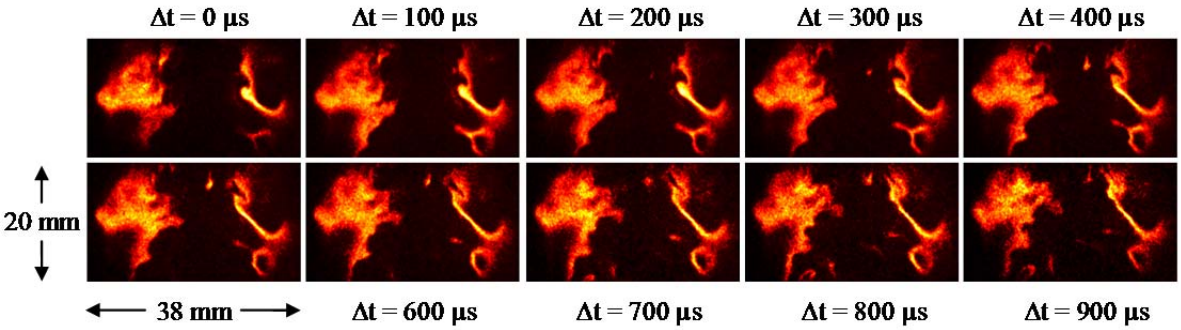

Fig. 11: 10-kHz sequence of the CH_2O field in a turbulent non-premixed CH_4 flame (Re = 6000). Images are centered at x/d = 8.

combustion chemistry and plays a crucial role in ignition and unwanted processes such as "knock". Measurements of CH_2O fluctuations allow an examination of the effects of the highly intermittent turbulent flowfield on the low-temperature chemistry which includes fuel oxidation and ignition processes. An example set of 10-kHz CH_2O PLIF images acquired using a PBLS in a turbulent CH_4 jet flame (Re = 6000) are shown in Fig. 11 and were first reported in Ref. 30. The measurements were acquired with approximately 100 mJ/pulse at 355 nm (3^{rd} harmonic output of the PBLS). Future work includes using high-speed CH_2O PLIF to understand auto-ignition dynamics and the temporal evolution of low-temperature chemistry in turbulent flames using alternative fuels such as dimethyl ether.

IV. References

1. Böhm, B., Heeger, C., Gordon, R.L., Dreizler, A., New Perspectives on Turbulent Combustion: Multi-Parameter High-Speed Planar Laser Diagnostics, *Flow Turbulence and Combustion* 2011, 86(3-4), 313-341.
2. Barlow, R.S., Laser Diagnostics and Their Interplay with Computations to Understand Turbulent Combustion, *Proceedings of the Combustion Institute* 2007, 31(1) 49-75.
3. Thurow, B.S., Jiang, N., Lempert, W.R., Review of ultra-high repetition rate laser diagnostics for fluid dynamic measurements , *Measurement, Science, and Technology* 2013, 24 012002.
4. Fuest, F., Papageorge, M.J., Lempert, W.R., Sutton, J.A., Ultra-High Laser Pulse Energy and Power Generation at 10 kHz, *Optics Letters*, 2012, 37(15), 3231-3233.
5. Hunt, J.T., Glaze, J.A., Simmons, W.W., Renard, P.A., Suppression of self-focusing through low-pass spatial filtering and relay imaging, *Applied Optics*, 1978, 17(13), 2053-2057.
6. Thurow, B.S., Jiang, N., Samimy, M., Lempert, W.R., Narrow-Linewidth Megahertz-Rate Pulse-Burst Laser for High-Speed Flow Diagnostics, *Applied Optics* 2005, 43(26), 5064.

7. Buch, K.A., Dahm, W.J.A., Experimental Study of the Fine-Scale Structure of Conserved Scalar Mixing in Turbulent Shear Flows. Part 2. $Sc \approx 1$. *Journal of Fluid Mechanics* 1998, 364, 1-29.

8. Su, L.K., Clemens, N.T., Planar Measurements of the Full Three-Dimensional Scalar Dissipation Rate in Gas-Phase Turbulent Flows. *Experiments in Fluids* 1999, 27, 507-521.

9. Su, L.K., Clemens, N.T., The Structure of Fine-Scale Scalar Mixing in Gas-Phase Planar Turbulent Jets. *Journal of Fluid Mechanics* 2003, 488, 1-29.

10. Patton, R.A., Gabet, K.N., Jiang, N., Lempert, W.R., Sutton, J.A., Multi-kHz Mixture Fraction Imaging in Turbulent Jets Using Planar Rayleigh Scattering, *Applied Physics B*, 2011, 106(2), 457-471.

11. Hain, R., Kahler, C.J., Tropea, C., Comparison of CCD, CMOS, and Intensified Cameras. *Experiments in Fluids* 2007, 42, 403-411

12. Weber, V., Brubach, J., Gordon, R.L., Dreizler, A., Pixel-Based Characterisation of CMOS High-Speed Camera Systems, *Applied Physics B* 2011, 103, 421-433.

13. Papageorge, M.J. McManus, T.A., Fuest, F., Sutton, J.A., Recent Advancements in High-Speed Planar Rayleigh Scattering Imaging: Increased Record Lengths, Repetition Rates, and Spatial Resolution, to be submitted to Applied Physics B, 2013.

14. Tacina, K.M. and Dahm, W.J.A., Effects of heat release on turbulent shear flows. Part 1. A general equivalence principle for nonbuoyant flows and its application to turbulent jet flames. *Journal of Fluid Mechanics*, 2000, 415, 23 - 44.

15. Wang, G.H., Clemens, N.T., Varghese, P.L., High-Repetition Rate Measurements of Temperature and Thermal Dissipation in a Non-premixed Turbulent Jet Flame, *Proceedings of the Combustion Institute* 2005, 30, 691-699.

16. Everest, D., Driscoll, J.F., Dahm, W.J.A. and Feikema, D., Images of the 2-DTemperature Field and Temperature Gradients to Quantify Mixing Rates Within a Non-Premixed Turbulent Jet Flame, *Combustion and Flame* 1995, 100, 58-69.

17. Patton, R.A., Gabet, K.N., Jiang, N., Lempert, W.R., Sutton, J.A., Multi-kHz Temperature Imaging in Turbulent Nonpremixed Flames Using Planar Rayleigh Scattering, *Applied Physics B*, 2012 108(2), 377-392.

18. Meier, W., Barlow, R.S., Chen, Y.L., Chen, J.Y., Raman/Rayleigh/LIF Measurements in a Turbulent $CH_4/H_2/N_2$ Jet Diffusion Flame: Experimental Techniques and Turbulence-Chemistry Interaction, *Combustion and Flame* 2000, 123(3), 326.

19. Bergmann, V., Meier, W., Wolff, D., Stricker, W., Application of Spontaneous Raman and Rayleigh Scattering and 2D LIF for the Characterization of a Turbulent CH4/H2/N2 Jet Diffusion Flame, *Applied Physics B-Lasers and Optics* 1998, 66(4), 489.

20. Barlow, R.S., International Workshop on Measurement and Computation of Turbulent Nonpremixed Flames, http://www.ca.sandia.gov/TNF/abstract.html

21. Bilger, R.W., Turbulent Diffusion Flames, *Progress in Energy and Combustion Science*, 1976, 1, 87.

22. Gabet, K.N., Jiang, N., Patton, R. A., Lempert, W.R,. Sutton, J.A. ,Demonstration of High-Speed 1D Raman Scattering Line Imaging, *Applied Physics B*, 101 (1-2) (2010) 1-5.

23. Jiang, N., Lempert, W.R., Switzer, G.L., Meyer, T.R., Gord, J.R., Narrow-Linewidth Megahertz-Repetition-Rate Optical Parametric Oscillator for High-Speed Flow and Combustion Diagnostics, *Applied Optics* 2008 47(1), 64-71.

24. Jiang, N., Lempert, W.R., "Ultra-High Frame Rate Nitric Oxide Planar Laser Induced Fluorescence Imaging", *Optics Letters*, Vol. 33, No. 19, 2008, p. 2236.

25. Jiang, N., Webster, M. , Lempert, W.R. ,New advances in generation of high repetition rate burst mode laser output, *Applied Optics*, 2009, 48 (4), B23-31.

26. Jiang, N., Bruzzese, J., Patton, R., Sutton, J.A., Yentsch, R., Gaitonde, D.V, Lempert, W.R., Miller, J.D., Meyer, T.R., Parker, R., Wadham, T., Holden, M., Danehy, P.M., "NO PLIF Imaging in the CUBRC 48-Inch Shock Tunnel," *online, Experiments in Fluids*, 2012, DOI: 10.1007/s00348-012-1381-6

27. Miller, J.D., M. Slipchenko, T. R. Meyer, N. Jiang, W. R. Lempert , J. R. Gord , Ultrahigh-frame-rate OH fluorescence imaging in turbulent flames using a burst-mode optical parametric oscillator, *Optics Letters* 2009, 34(9), 1309-1311.

28. Jiang, N., Patton, R.A., Lempert, W.R., Sutton, J.A., Development of High-Repetition Rate CH PLIF Imaging in Turbulent Nonpremixed Flames, *Proceedings of the Combustion Institute* 2010, 31(1), 767-774.

29. Donbar, J.M., Driscoll, J.F., Carter, C.D., Reaction Zone Structure in Turbulent Nonpremixed Jet Flames – From CH-OH PLIF Images, *Combustion and Flame* 2000, 122(1-2), 1.

30. Gabet, K.N., Patton, R.A., Jiang, N., Lempert, W.R., Sutton, J.A., High-Speed CH_2O PLIF Imaging in Turbulent Flames Using a Pulse Burst Laser System, *Applied Physics B*, 2012 106(3), 569-575.

V. Personnel Supported

Jeffrey A. Sutton, Principle Investigator

Randy Patton, Current Graduate Student

Thomas McManus, Current Graduate Student

Michael Papageorge, Current Graduate Student

VI. Additional Personnel (No Cost)

Walter R. Lempert, Collaborator, Professor, Ohio State University

Kathryn Gabet, Current Graduate Student

VII. Journal Publications Resulting from AFOSR-Supported Work

Fuest, F., Papageorge, M.J., Lempert, W.R., Sutton, J.A., "Ultra-High Laser Pulse Energy and Power Generation at 10 kHz," *Optics Letters*, 2012, 37(15), 3231-3233.

Jiang, N., Bruzzese, J., Patton, R., Sutton, J.A., Yentsch, R., Gaitonde, D.V, Lempert, W.R., Miller, J.D., Meyer, T.R., Parker, R., Wadham, T., Holden, M., Danehy, P.M., "NO PLIF Imaging in the CUBRC 48-Inch Shock Tunnel," *online*, *Experiments in Fluids*, 2012, DOI: 10.1007/s00348-012-1381-6

Patton, R.A., Gabet, K.N., Jiang, N., Lempert, W.R., Sutton, J.A., "Multi-kHz Temperature Imaging in Turbulent Non-premixed Flames Using Planar Rayleigh Scattering", *Applied Physics B*, 2012,108(2), 377-392.

Gabet, K.N., Patton, R.A., Jiang, N., Lempert, W.R., Sutton, J.A., "High-Speed CH_2O PLIF Imaging in Turbulent Flames Using a Pulse Burst Laser System", *Applied Physics* 2012, 106(3), 567-575.

Patton, R.A., Gabet, K.N., Jiang, N., Lempert, W.R., Sutton, J.A., "Multi-kHz Mixture Fraction Imaging in Turbulent Jets Using Planar Rayleigh Scattering", *Applied Physics B*, 2011, 106(2), 457-471.

Jiang, N., Patton, R.A., Lempert, W.R., Sutton, J.A., "Development of High-Repetition Rate CH PLIF Imaging in Turbulent Nonpremixed Flames", *Proceedings of the Combustion Institute*, 2011, 33(1), 767-774.

Gabet, K.N., Jiang, N., Lempert, W.R., Sutton, J.A., "Demonstration of High-Speed 1D Raman Scattering Line Imaging", *Applied Physics B* 2010, 101 (1-2), 1-5.

VIII. Conference Presentations during Reporting Period

Papageorge, M.J., Fuest, F., Sutton, J.A., "Time-Resolved, Two-Dimensional Imaging of Scalar Mixing in Turbulent Gas-Phase Jets," 65th Annual Meeting of the Division of Fluid Dynamics, American Physical Society, San Diego, CA, 2012

McManus, T.A., Papageorge, M.J., Fuest, F., Sutton, J.A., "Recent Advances in kHz-Rate Imaging Using a Next-Generation Pulse Burst Laser System: Increased Signal-to-Noise, Repetition Rates, Record Lengths, and Spatial Resolution," Work-in-Progress Poster Presentation, 34th *International Symposium on Combustion*, Warsaw, Poland, 2012.

Gabet, K.N., Fuest, F., Sutton, J.A., "Quantification and Accuracy of a CMOS-Based Raman Scattering Imaging System for High-Speed Measurements in Flames," Work-in-Progress Poster Presentation, 34th *International Symposium on Combustion*, Warsaw, Poland, 2012.

Papageorge, M., Lempert, W.R., Sutton, J.A., "Development of a Next-Generation Pulse Burst Laser System for Time-Resolved Fluid Dynamics and Combustion Measurements", *50th Aerospace Sciences Meeting*, Nashville, TN, January, 2012.

Gabet, K.N., Jiang, N., Lempert, W.R., Sutton, J.A., "Development of High-Speed Raman Scattering Imaging in Flames", *16th Gordon Research Conference on Laser Diagnostics in Combustion*, Waterville Valley, NH, 2011.

Gabet, K.N, Jiang, N., Lempert, W.R., Sutton, J.A., "Towards High-Speed 1D Raman Scattering Line Imaging in Turbulent Flames", *7th U.S. National Combustion Meeting*, Atlanta, GA, March, 2011.

Patton, R.A., Gabet, K.N., Jiang, N., Lempert, W.R., Sutton, J.A. "Further Development of High-Speed Rayleigh and Raman Scattering Imaging in Turbulent Jets and Flames", Work-in-Progress Poster Presentation, 33rd *International Symposium on Combustion*, Beijing, China, 2010.

Gabet, K.N., Jiang, N., Lempert, W.R., Sutton, J.A, "Towards the Development of High-Speed 1-D Raman Scattering in Turbulent Non-Premixed Flames", *49th Aerospace Sciences Meeting*, Orlando, FL, January 2011.

Patton, R.A., Jiang, N., Lempert, W.R., Sutton, J.A., "Towards Simultaneous High-Speed Mixture Fraction and Velocity Imaging in Turbulent Jets", *49th Aerospace Sciences Meeting*, Orlando, FL, January 2011.

Jiang, N., Bruzzese, J., Patton, R., Sutton, J.A., Lempert, W., Miller, J., Meyer, T., Parker, R., Danehy, P., "NO PLIF Imaging in the CUBRC 48" Shock Tunnel", *49th Aerospace Sciences Meeting*, Orlando, FL, January 2011.

Sutton, J.A., Gabet, K.N., Patton, R.A. Jiang, N.B., Lempert, W.R., "Towards High-Repetition-Rate Rayleigh and Raman Scattering Imaging in Turbulent Jets and Flames", *48th Aerospace Sciences Meeting*, Orlando, FL, January 2010.

Sutton, J.A., Gabet, K.N., Patton, R.A., Jiang, N., Lempert, W.R., "From Hz to kHz: Development of High-Repetition Rate Rayleigh and Raman Scattering Diagnostics", *15th Gordon Research Conference on Laser Diagnostics in Combustion*, Waterville Valley, NH, 2009.

IX. Invited Presentations/Seminars

Sutton, J.A., "An Introduction to the Activities within the Turbulence and Combustion Research Laboratory at OSU", AIAA, Aerodynamic Measurement Technology Technical Committee meeting, 2012.

Sutton, J.A., Lempert, W.R., "Advances in High-Energy, High-Repetition Rate Diagnostics for PLIF, Rayleigh, and Raman Scattering Imaging in Turbulent Reacting Flows", *49th Aerospace Sciences Meeting*, Orlando, FL, January 2011

Jiang, N.B., Webster, M.C., Gabet, K.N., Patton, R.A., Miller, J.D., Meyer, T.R., Inman, J.A., Bathel, B., Jones, S.B., Danehy, P.M., Adamovich, I.V., Sutton, J.A., Lempert, W.R., "Ultra High Framing-Rate Laser Diagnostics for High-Speed Reacting and Non-Reacting Flows", *LACSEA*, San Diego, CA, January, 2010

Sutton, J.A., "From Hz to kHz: Development and Application of High-Pulse-Energy, High-Speed Laser Diagnostics in Turbulent Reacting Flows", 16th Gordon Research Conference on Laser Diagnostics in Combustion, 2011.

Sutton, J.A., "New Developments in High-Energy, High-Repetition Rate Laser Diagnostics for Multi-kHz PLIF, Rayleigh and Raman Scattering Measurements in Turbulent Reacting Flows", School of Aerospace Engineering, Georgia Institute of Technology, 2011.

Sutton, J.A., "New Developments in High-Energy, High-Repetition Rate Laser Diagnostics for Multi-kHz PLIF, Rayleigh and Raman Scattering Measurements in Turbulent Combustion

Environments", Department of Mechanical and Aerospace Engineering, University of Virginia, 2011.

Sutton, J.A., "New Developments in High-Energy, High-Repetition Rate Laser Diagnostics for Multi-kHz Measurements in Turbulent Reacting Flows", Department of Mechanical and Aerospace Engineering, Cornell University, 2011.

Sutton, J.A., "Advanced Laser Diagnostics for Understanding Combustion Dynamics, Stability, and Extinction in Laboratory-Scale Flames", Department of Aerospace and Astronautical Engineering, The Ohio State University, 2009.

X. Honors and Awards during Reporting Period

National Science Foundation Faculty Early Career (CAREER) Award, 2011

American Chemical Society Petroleum Research Fund New Doctoral Investigator Award, 2010

Naval Research Laboratory, Chemistry Division Award for Research and Technical Writing, 2010